Bifurcation, chaos, modulation instability, and soliton analysis of the Schrödinger equation with cubic nonlinearity

[1]Md. Shahidur Rahaman, [1]Mohammad Nazrul Islam, [2,*]Mohammad Safi Ullah

[1]Department of Mathematics, Jahangirnagar University, Dhaka-1342, Bangladesh
rahamans761@gmail.com (M. S. Rahaman), islamju@juniv.edu (M. N. Islam)
[2]Department of Mathematics, Comilla University, Cumilla-3506, Bangladesh
safi.ru1985@gmail.com (M. S. Ullah)

[*]**Corresponding Author:** safi.ru1985@gmail.com (M. S. Ullah)

Abstract

Bifurcation, chaos, modulation instability, and solitons are important phenomena in nonlinear dynamical structures that help us understand complex physical processes. This work employs the Schrödinger equation with cubic nonlinearity (SECN), rising in superconductivity, quantum mechanics, optics, and plasma physics. We developed an ordinary differential arrangement using a traveling wave alteration and found the soliton outcome to the mentioned problem utilizing the unified solver technique. Then we obtain different categories of wave designs, including bright and dark solitons, with periodic, quasiperiodic, and chaotic behaviors. We examined the system's planar dynamics to observe sensitivity, chaos, and bifurcation. The chaotic state involves various procedures such as multistability, recurrence diagrams, bifurcation shapes, fractal dimensions, return maps, Poincaré graphics, Lyapunov exponents, phase portraits, and strange attractors. These properties help us understand complicated behaviors like how waves become chaotic patterns. Our outcomes demonstrate a clear understanding of wave propagation and how energy is absorbed. These findings develop our knowledge of nonlinear problems and guide us in wave circulation in real-life situations. Therefore, our procedures are useful and operative offering a simple technique for studying nonlinear problems, which progresses our understanding of these equations' sensitivity, waveform pattern, and propagation strategy.

Keywords: Unified solver procedure, sensitivity assessment; Lyapunov exponent; stranger attractor; basins of attraction; dynamical system.

1. Introduction

The study of many dynamical happenings in the real world, especially in the domains of chemical reactions [1], plasma physics [2], magnetohydrodynamics [3], optical fibers [4], fluid dynamics [5], telecommunications [6], quantum mechanics [7], and other applications [8-10], depends heavily on nonlinear evolution equations. Nonlinear science is witnessing the emergence of numerous well-known nonlinear models, including the generalized Kudryashov's system [11], the generalized nonlinear Schrödinger equation with nonlocal effect [12], the nonlinear Schrödinger equation with the Kerr effect [13], the longitudinal wave equation [14], the Kolmogorov-Petrovsky-Piskunov form [15], the Zoomeron equation [16], the Phi-4 nonlinear structure [17], the Hirota-Maccari system [18], the KFG equation [19], the new Hamiltonian amplitude model [20], and others. Researchers have been working hard to explore these nonlinear equations in recent years. Since precise solutions to these equations are crucial for understanding different dynamic processes in the real world, there is a thriving field of research with encouraging findings. There are many ways to get exact answers to these equations, such as the unified solver method [21], the generalized Ricatti equation mapping technique [22], the novel modified Kudryashov scheme [23], the unified process [24], and more.

Bifurcation analysis is a suitable technique for examining dynamic patterns and has significant usage in numerous fields [25]. It is a crucial instrument for assessing nonlinear models' dynamics. This technique is employed for examining the chaotic dynamics, sensitivity examination, multistability, and soliton solutions, investigating how altering the system's parameters impacts the qualitative elements [26]. Researchers can use bifurcation analysis to examine the change from steady to unsteady situations. It is a valuable tool for evaluating and understanding how complex systems behave.

This study develops soliton solutions using the unified solver method and planner dynamics, revealing the chaotic state corresponding to Eq. (1). We include modulation instability, which leads to dispersion and nonlinear impacts in various nonlinear systems. We also discover and study chaos using multistability, fractal dimensions, strange attractors, recurrence maps, return diagrams, Poincaré illustrations, bifurcation plots, Lyapunov exponents, 3D and 2D phase representations, and recurrence diagrams. These types of studies have not yet examined the underlying model of these processes. This work helps us understand how nonlinear waves behave by carefully studying soliton solutions, bifurcations, and chaos in the governing equation. Unlike previous studies, this one uses the advanced tools described above to explain nonlinear instabilities. These discoveries improve wave control and predictability, providing useful information for quantum mechanical, plasma physics, and optical applications.

Here is the plan for the research project: The Schrödinger system's mathematical structure is explained in Section 2. Section 3 demonstrates the application of unified solver approaches. Section 4 contains a graphic representation. Section 5 presents the bifurcation evaluation. Section 6 depicts chaotic behaviors. Section 7 presents the sensitivity investigation of the expected nonlinear problem. Section 8 presented the study of multistability. In Section 9, the chaotic pattern is presented together with other features. Section 10 presents an analysis of modulation instability in the suggested model. Section 11 presents a comparison and highlights the novel results. Section 12 highlights the limitations and future work opportunities. Finally, the results of this investigation are presented in Section 13.

2. The governing model

The nonlinear Schrödinger equation is a partial differential equation applicable to classical and quantum mechanics. The main uses of this classical field equation are in planar waveguides and nonlinear optical fibers for light transmission. Erwin Rudolf Josef Alexander Schrödinger, an Austrian physicist who formulated the Schrödinger equation in 1925 and published it in 1926, is sometimes referred to as Schrödinger or Schrödinger. His work served as the foundation for research, earning him the Nobel Prize in physics in 1933. We can study quantum mechanical structures and make predictions in ways beyond the Schrödinger equation. Richard Feynman's route integral structure and Werner Heisenberg's matrix mechanics are different ways to formulate quantum mechanics. The Schrödinger equation, also known as wave mechanics, is a relativistic variant of the Klein-Gordon equation, resulting in nonrelativistic space and time relationships. Its applications include quantum computing, plasma control, and optical communications, making it appealing to a wider audience. Emphasizing relevant applications would help appeal to a wider audience. We write the Schrödinger equation with cubic nonlinearity as follows [27]:

$$iw_t + w_{xx} + |w|^2 w = 0. \tag{1}$$

Here W represents a wave function, W_{xx} represents the dispersion. To obtain the soliton solutions of the SECN, we introduce:

$$w(x,t) = W(S)e^{i\theta}, S = x - at, \theta = bx + dt, \tag{2}$$

where a and θ are the wave velocity and wavenumber, sequentially. By employing Eq. (2) in Eq. (1), we calculate that $a = 2b$ and W fulfill the following

$$W''(S) + W^3(S) - (d + b^3)W(S) = 0. \tag{3}$$

3. Implementation of the unified solver procedure

The unified solver procedure can get the soliton answers to difficult nonlinear problems, even the conformable nonlinear stochastic model [28]. However, it is challenging to solve traditional approaches. The method is simple and qualified for various nonlinear difficulties. With this method, researchers can get different soliton results, such as trigonometric, hyperbolic, rational, periodic, double-periodic, and breather wave results [19, 21, 28]. This procedure suggests more exact and sophisticated solutions than the traditional procedure, making it more appropriate for complicated nonlinear problems.

We present a precise solution to the equation that follows [19, 21, 28]:

$$\lambda W''(S) + \eta W^3(S) + HW(S) = 0. \tag{4}$$

The result of Eq. (1) is as follows:

(i) Rational type: (where $H = 0$)

$$W_{1,2}(S) = \left(\mp\sqrt{\frac{-\eta}{2\lambda}}(g+S)\right)^{-1}. \tag{5}$$

(ii) Trigonometric type: (where $\frac{H}{\lambda} > 0$)

$$W_{3,4}(S) = \left(\pm\sqrt{\frac{H}{\eta}}\tan\left(\sqrt{\frac{-H}{2\lambda}}\right)(g+S)\right) \tag{6}$$

and

$$W_{5,6}(S) = \left(\pm\sqrt{\frac{H}{\eta}}\cot\left(\sqrt{\frac{-H}{2\lambda}}\right)(g+S)\right). \tag{7}$$

(iii) Hyperbolic type: (where $\frac{H}{\lambda} < 0$)

$$W_{7,8}(S) = \left(\pm\sqrt{\frac{-H}{\eta}}\tanh\sqrt{\frac{H}{2\lambda}}(g+S)\right) \tag{8}$$

and

$$\mathrm{W}_{9,10}(S) = \left(\pm \sqrt{\frac{-H}{\eta}} \coth \sqrt{\frac{H}{2\lambda}} (g+S) \right), \tag{9}$$

where g is any arbitrary constant. From Eq. (3) and Eq. (4), we obtain $H = -(d+b^3)$, $\lambda = 1, \eta = 1$. Following this, by applying Eq. (2) and the unified solver approach, we arrive at

(i) Rational type: (where $H = 0$)

$$w_{1,2}(x,t) = \left(\mp \sqrt{\frac{-1}{2}} (g+x-2bt) \right)^{-1} e^{i\,(bx+dt)}. \tag{10}$$

(ii) Trigonometric type: (where $\frac{H}{\lambda} > 0$)

$$w_{3,4}(x,t) = \left(\pm \sqrt{-(d+b^3)} \tan \left(\sqrt{\frac{(d+b^3)}{2}} \right) (g+x-2bt) \right) e^{i\,(bx+d\ )} \tag{11}$$

and

$$w_{5,6}(x,t) = \left(\pm \sqrt{-(d+b^3)} \cot \left(\sqrt{\frac{d+b^3}{2}} \right) (g+x-2bt) \right) e^{i\,(bx+dt)}. \tag{12}$$

(iii) Hyperbolic type: (where $\frac{H}{\lambda} < 0$)

$$w_{7,8}(x,t) = \left(\pm \sqrt{d+b^3} \tanh \left(\sqrt{-\frac{d+b^3}{2}} \right) (g+x-2bt) \right) e^{i\,(bx+d\ )} \tag{13}$$

and

$$\mathrm{w}_{9,10}(x,t) = \left(\pm \sqrt{d+b^3} \coth \left(\sqrt{-\frac{d+b^3}{2}} \right) (g+x-2bt) \right) e^{i\,(bx+dt)}, \tag{14}$$

where b, d, and g are arbitrary constants.

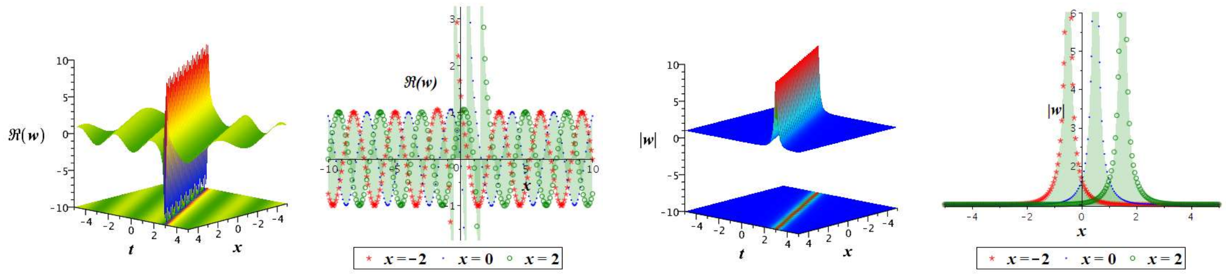

(a) (b) (c) (d)

Fig 1. Diagram for Eq.(12) with $b = g = e = 1$, and $d = -2$. (a, b): Periodic breathers with singularity, and (c, d): bright soliton with singularity.

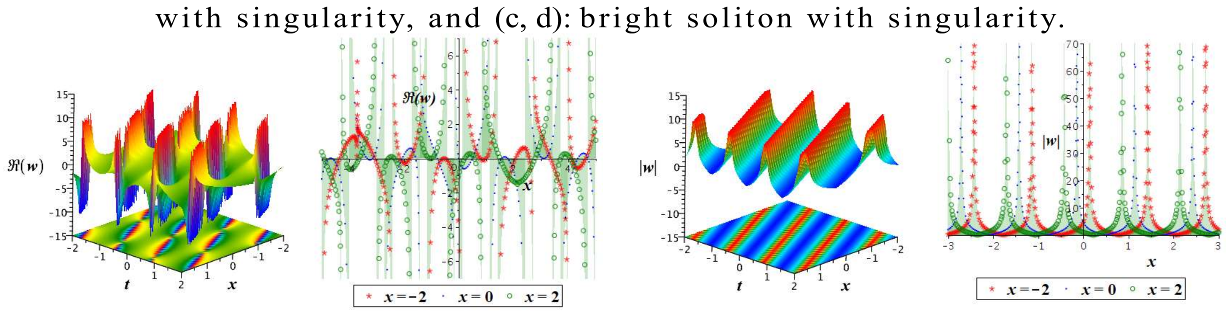

(a) (b) (c) (d)

Fig 2. Diagram for Eq.(13) with $b = g = e = 1$, and $d = 2$. (a, b): Multiple breather waves with singularity, and (c, d): periodic waves with singularity.

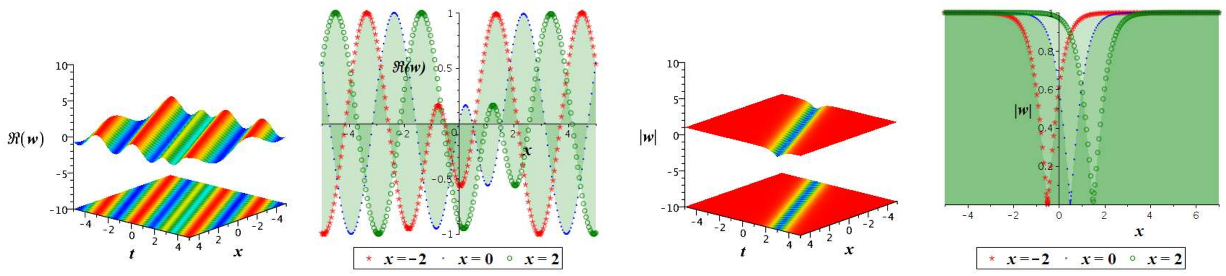

(a) (b) (c) (d)

Fig 3. Diagram for Eq.(11) with $b = g = e = 1$, and $d = -2$. (a, b): Double periodic wave, and (c, d): dark soliton.

4. Graphical explanation

The governing model's visual illustration for several parameter values—b, d, e, and g—is highlighted in the current section. Solutions w_1, w_2, w_5, and w_6 represent analogous nature as plotted in **Fig.1** by w_5 for $b = g = e = 1$, and $d = -2$. $Re(w_5)$ is shown in Figures **1a** and **1b**, where it looks like a singular waveform with periodic breathers. $abs(w_5)$ is shown in Figures **1c** and **1d**, which are bright solitons and contain a singularity. The behavior of w_7, w_8, w_9, and w_{10}

is equivalent to that of w_7 depicted in **Fig. 2** for $b = g = e = 1, d = 2$. $Re(w_7)$ is discovered in Fig. 2a, and 2b which signifies multi-breathers with bright dark waveforms and $abs(w_7)$ is exhibited in Fig. 2c, 2d, which illustrate a periodic wave with singularity. w_3 and w_4 signify similar patterns as pictured in Fig.3 by w_3 for $b = g = e = 1, d = -2$. $Re(w_3)$ is depicted in Fig. 3a, 3b, which represents double periodic solitons and $abs(w_3)$ corresponds to Fig. 3c and 3d denotes dark soliton.

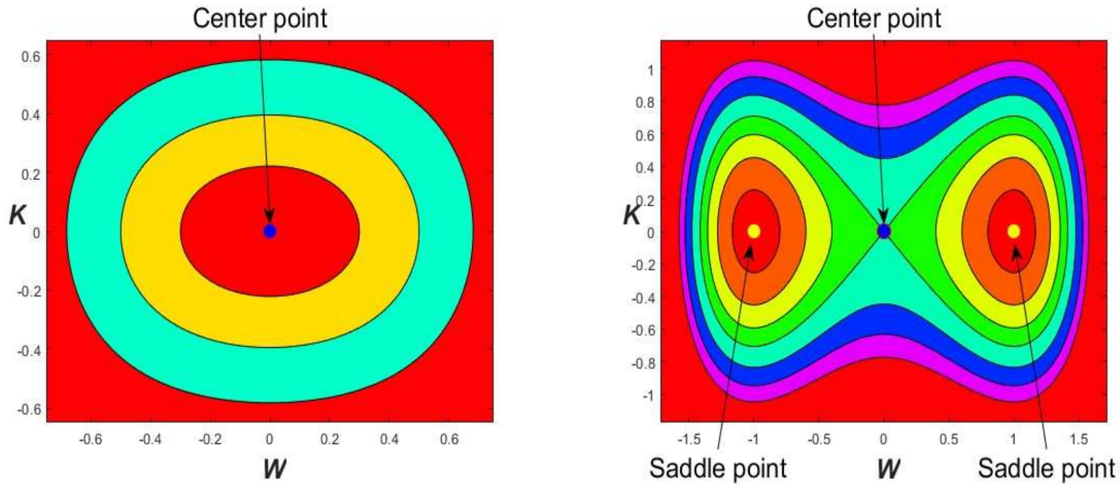

Fig 4. Phase portrait for Eq.(15) with (a) $b = 1$ and $d = 2$, (b) $b = 1$ and $d = 2$.

5. Bifurcation analysis

Bifurcation arises in dynamic systems when the system exhibits qualitative behavior due to small changes in parameter settings [29-31]. It can lead to periodic orbits, unpredictable behavior, and new stable phases. The bifurcation hypothesis explains these unexpected events as well as predicts how structures will behave at different stages of their evolution [32]. One example of bifurcation in a real-world system is the transition between different traffic flow patterns on a highway. As the density of vehicles increases, the system can shift from free-flowing traffic to congested stop-and-go waves. This change represents a bifurcation, where a small increase in cars leads to a significant alteration in traffic behavior. This section compiles the phase diagrams for the next planned dynamical form. This method enables narrative analysis of nonlinear systems.

Let $\frac{dW}{ds} = K$, the planner dynamics of the governing problem for equation Eq.(3) can be stated as below:

$$\frac{dW}{ds} = K, \quad \frac{dK}{ds} = -W^3 + (d + b^3)W. \tag{15}$$

From the first integration for Eq.(15), one reaches the subsequent Hamiltonian functions

$$H(W, K) = \frac{1}{2}K^2 + \frac{1}{4}W^4 - \frac{(d+b^3)}{2}W^2 = h, \tag{16}$$

which satisfies the Hamiltonian canonical formulation $W' = \frac{\partial \mathrm{H}}{\partial \mathrm{K}}$, $K' = -\frac{\partial \mathrm{H}}{\partial \mathrm{W}}$, where h characterizes a continuous variable, also called the Hamiltonian constants or energy levels. Moreover, $\frac{1}{2}K^2$ denotes the kinetic energy, and $\frac{1}{4}W^4 - \frac{(d+b^3)}{2}W^2$ represents the potential energy for the Hamiltonian Eq.(16).

Case 1: $d + b^3 > 0$.

Fig.4a displays the three EPs $(-1,0)$, $(0,0)$, and $(1,0)$, which are accessible across the following limit settings: $b = 1$ and $d = -1.5$. It is evident from the graphic that $(0, 0)$ denotes a center, but $(1, 0)$ and $(-1, 0)$ are recognized as saddle kinds. **Fig.4a** shows kink wave and anti-kink features, created by combining different paths called heteroclinic routes: $(-1, 0)$ and $(1, 0)$.

Case 2: $d + b^3 < 0$.

The variable settings are shown here, $b = -1$ and $d = 2$, can only yield an EP of $(0, 0)$; **Fig.4b** illustrates this. The graphic shows what happens when we represent a saddle point as $(0, 0)$. The closed loops of the framework are not included in the pathways.

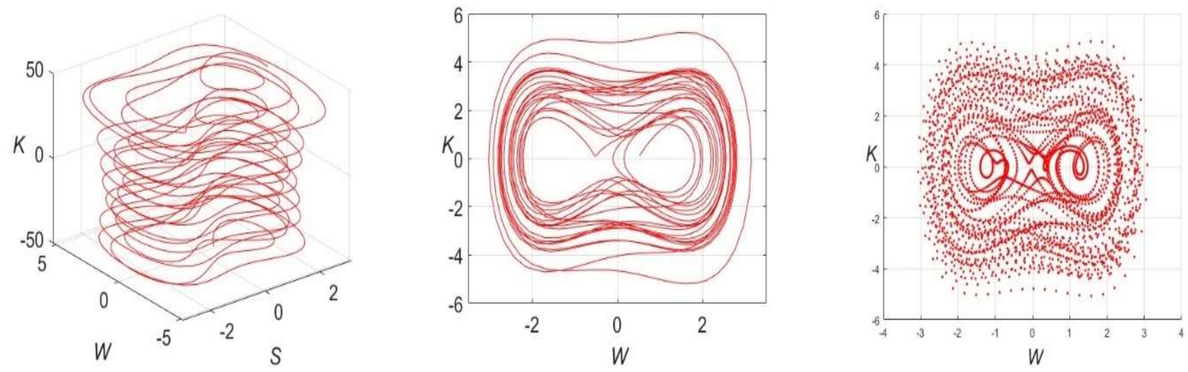

(a) 3D phase plot (b) 2D phase plot (c) Poincaré plot

Fig 5. Chaotic characteristics of Eq.(17) with $b = d = 1$, $\alpha = 1.3$, and $\rho = 1.3$.

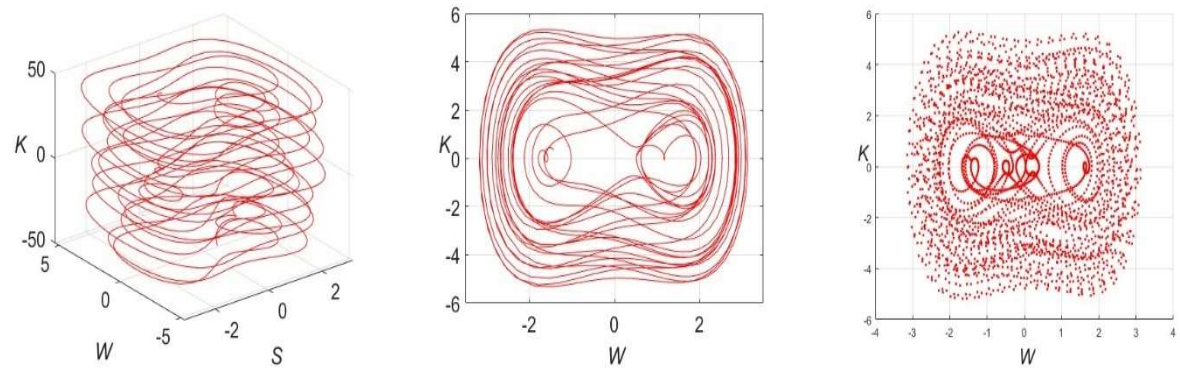

(a) 3D phase plot (b) 2D phase plot (c) Poincaré plot

Fig 6. Chaotic characteristics of Eq.(17) with $b = d = 1$, $\alpha = 1.5$, and $\rho = 1.3$.

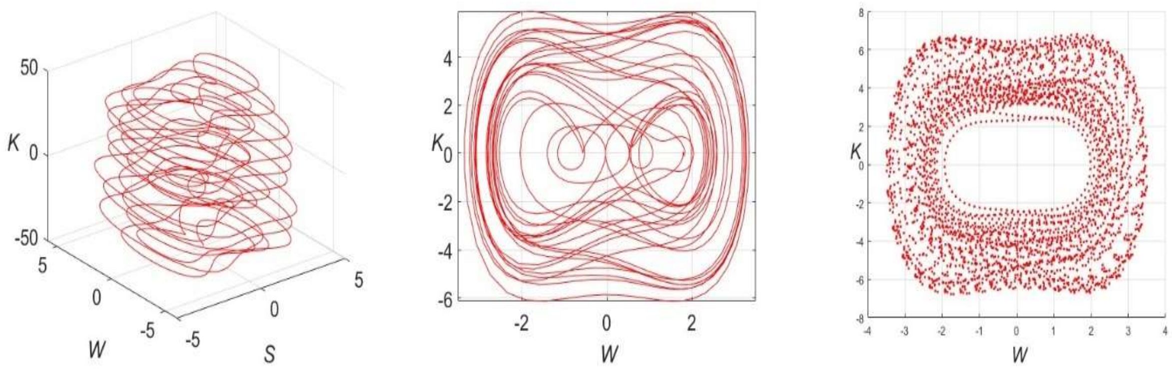

(a) 3D phase plot (b) 2D phase plot (c) Poincaré plot

Fig 7. Chaotic characteristics of Eq.(17) with $b = d = 1$, $\alpha = 2.5$, and $\rho = 1.3$.

6. Chaotic behaviors

Situations exhibiting seemingly random actions but controlled by irregular patterns are known as chaos [33]. Even slight variations in the starting values can result in wildly divergent long-term outcomes because chaotic structures are sensitive to initial conditions. Although geometries or structures often exhibit complicated and unexpected behaviors, these systems can uncover and explain them. Numerous man-made and natural systems, including optics, atmospheric circulation, and hydraulics, can display chaotic circumstances [34]. This segment explores the chaotic aspects of the resulting dynamic arrangement through an analysis of the damage format. This study includes a comparison of 2D and 3D stage layouts. To begin the analysis, look at another term in Eq.(9) that says

$$\frac{dW}{dS} = K, \frac{dK}{dS} = -W^3 + LW + \alpha \cos(\rho S), \tag{17}$$

in which $L = (d + b^3)$ with α and ρ correspond to amplitude and frequency, sequentially. We now examine how the system outlined in Eq.(17) is affected by the allotted frequency and strength. Keeping the essential factors constant ($b = d = 1$ and $\rho = 1.3$), different frequencies and intensity levels of chaotic designs are seen, as illustrated in **Fig. 5**, **Fig. 6**, and **Fig. 7** within the starting setting up $(0.52, 0.12)$. If $\alpha = 1.3$, the chaotic nature of Eq.(17) is exhibited in **Fig. 5a-5c**. For $\alpha = 1.5$, the chaotic nature of Eq.(17) is shown in **Fig 6a-6c**. For $\alpha = 2.5$, the chaotic nature of Eq.(17) is shown in **Fig. 7a-7c**.

7. Sensitivity analysis

The sensitivity analysis assesses the potential impact of varying input uncertainty on the output of a mathematical system [35]. Defining the elements that have the greatest impact on productivity and the distribution of input variations throughout the system is beneficial. Sensitivity analysis helps check if the expected results are reliable, consistent, and strong. This information is useful for making decisions about complicated systems [36]. This section describes how the starting conditions, set at $\rho = 1.3$ and $b = d = 1$, affect the disturbed form labeled by Eq. (17) at different strengths and frequencies. The red and blue lines in **Figs. 8a-8f** mark the locations of the final sequence of time images with the original designs $(0.52, 0.12)$ and $(0.52, 0.13)$, separately. In the absence of distribution intensities, the initial configuration of the disturbed form determines the periodic shape $(\alpha = 0)$ of the result, as shown in **Figs. 8a, d**. The blue and red sequence designs show relatively minor changes, indicating minimal sensitivity to the initial condition in cases when there is little quantity distributed $(\alpha = 1.5)$, as seen in **Figs. 8b, e**. Moreover, the period sequence plots show significant variations because of the increase in the perturbation's strength $(\alpha = 2.5)$, which is seen in **Figs. 8c, f**. This suggests that the initial conditions are extremely sensitive to modifications.

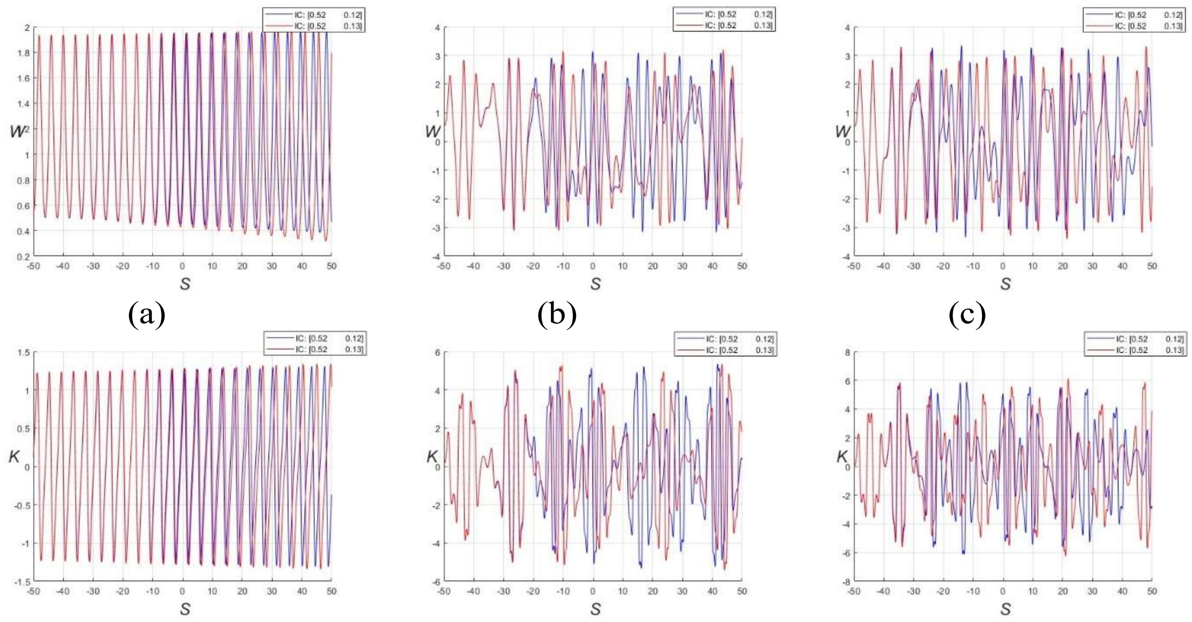

(a) (b) (c)

(d) (e) (f)

Fig 8: Sensitivity diagram within the framework Eq.(17) for $\rho = 1.3$ and $b = d = 1$: $\alpha = 0$ for (a, d), $\alpha = 1.5$ for (b, e), and $\alpha = 2.5$ for (c, f).

8. Multistability analysis

Multistability analysis [19] with influenced dynamical structures is the term used to describe a situation where many separate dynamic behaviors have the same set of parameters ($b = d = 1$, $\alpha = 2.5$, and $\rho = 1.3$) but different basic states. Periodicity, quasi-periodicity, chaos, multistability, and time series analysis, are among these behaviors that may appear in various circumstances. We have studied the multistability of the structure Eq.(17) in **Fig.9** and under different initial restrictions. Observations suggest that the system Eq.(17) is especially well-suited to chaotic initial conditions. It is simpler to describe and predict how complex dynamic systems will behave in different situations when one is aware of the properties of multistability, a key factor of these systems.

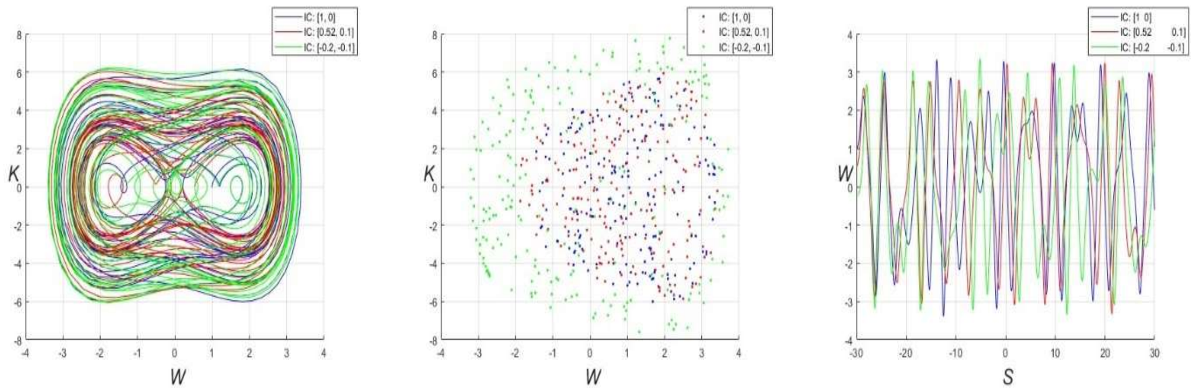

(a) 2D phase plot (b) Poincaré map (c) Time series plot

Fig 9: Multistability of Eq.(17) for $b = d = 1$, $\alpha = 2.5$, and $\rho = 1.3$.

9. Chaotic nature with other properties

Plotted in **Figs. 10, 11, 12, 13**, **14**, and **15**, this segment depicts the chaotic structure of the governing model under various situations [17, 21]. With beginning values of $(0.52, 0.12)$ and parameters $b = d = 1$, $\alpha = 2.5$, and $\rho = 1.3$, **Fig. 10** illustrates various chaotic features. **Fig. 10a** displays the fractal dimension design of the structure, which Eq. (17) represents. The image shows the chaotic feature of the model, displaying a fractal dimension of 0.98051, which is close to 1. The return map diagram of the structure characterized by Eq. (17) is shown in **Fig. 10b**. The figure's extensive dispersion indicates that the operational model is chaotic. We provide the power spectrum shape of the problem given by Eq. (17) in **Fig. 10c**. The recurrence graph of the system given by Eq. (17) is shown in **Fig. 11**. **Fig. 11a** displays recurrence graph about state variable W while **Fig. 11b** displays recurrence graph about state variable Q. The graphic indicates that the chosen model is chaotic due to the lack of regular diagonal lines or consistent structures. The ruling model's chaotic condition is evident from the figure's intricate, erratic design. The system, shown in **Fig. 12**'s bifurcation diagram, starts with the values $(0.52, 0.12)$ and uses the parameters $b = d = 1$, $\alpha = 2.5$, and $\rho = 1.3$ as described in Eq. (17). From **Fig. 12a**, we see that a single branch turns into many branches as the α value rises, illustrating the system's chaotic condition. Again, the discrete pattern of **Fig. 12b** shows the chaotic nature of the adopted model. The Lyapunov exponent diagram of the structure defined by Eq. (17) is shown in **Fig. 13a** and **13b**. The graphic indicates that a positive Lyapunov exponent is represented by the red curve, a negative Lyapunov exponent by the blue curve, and a zero Lyapunov exponent by the green curve. Being sensitive to initial input is an important feature of chaos. A positive Lyapunov exponent indicates that the model is chaotic. **Figs. 14a**, **14b**, and **14c** display the strange attractor diagrams of the system, which Eq. (17) gives with a delay of 5. The complicated, non-repeating pattern in the illustration adequately demonstrates the chaotic character of the proposed model. The basins of attraction for the system given by Eq. (17) are shown in **Fig. 15**. The picture demonstrates the chaotic character of the proposed model by clearly displaying the complex and imprecise borders of the basins.

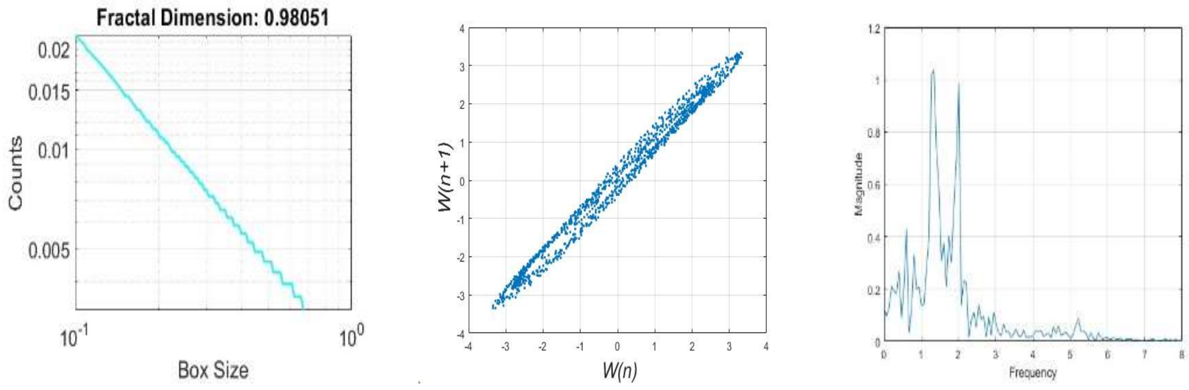

(a) Fractal dimension (b) Return map (c) Power spectrum plot

Fig 10: Various chaotic properties of Eq.(17) for $b = d = 1$, $\alpha = 2.5$, and $\rho = 1.3$ with beginning value $(0.52, 0.12)$.

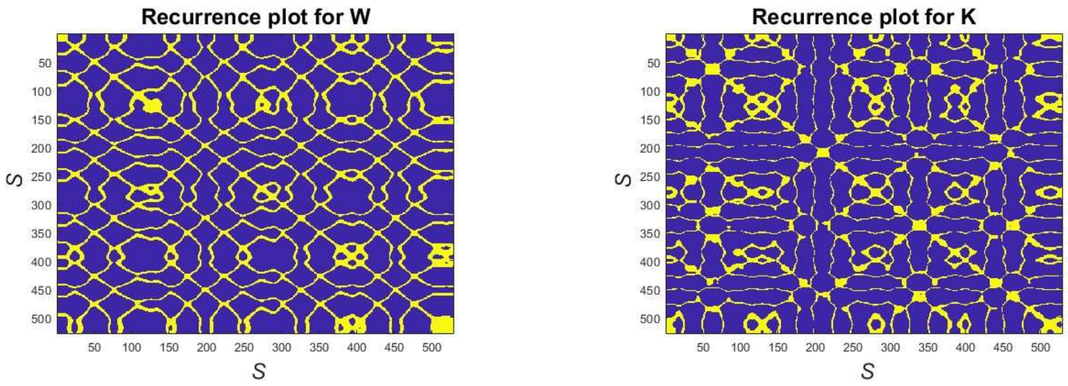

(a) (b)

Fig 11: Recurrence map of Eq.(17) for $b = d = 1$, $\alpha = 2.5$, and $\rho = 1.3$ with beginning value $(0.52, 0.12)$.

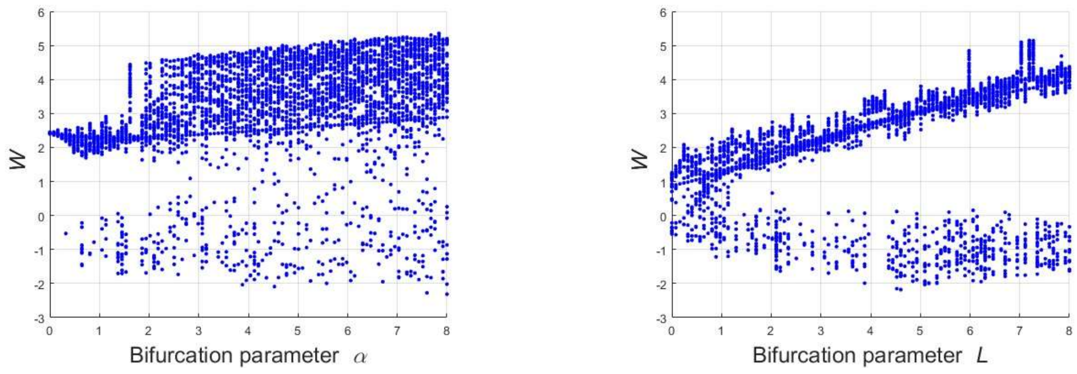

(a) (b)

Fig 12: Bifurcation plot of Eq.(17) for $b = 1$, $d = 2$, $\alpha = 2.5$, and $\rho = 1.3$ with the beginning value $(0.52, 0.12)$.

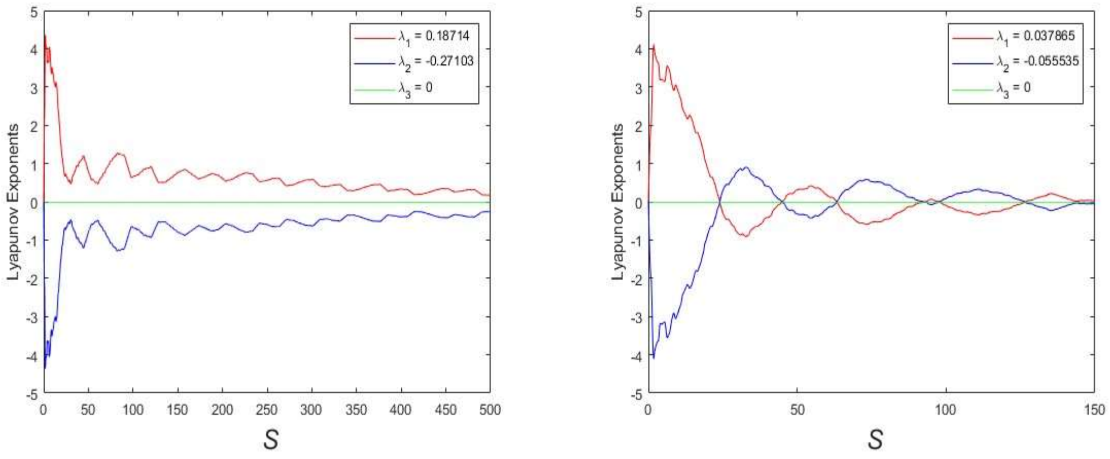

(a) (b)

Fig 13: Lyapunov exponent plot of Eq.(17) for $b = 1$, $d = 2$, and $\rho = 2.5$: (a) $\alpha = 1.3$ with initial value $(0.481, 0.001)$, (a) $\alpha = 1.28$ with initial value $(0.52, 0.0)$.

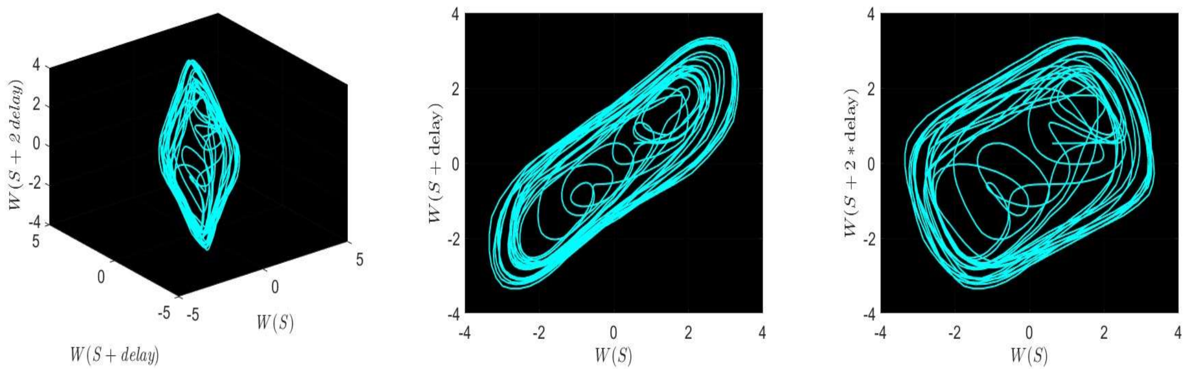

(a) 3D Strange attractor (b) 2D Strange attractor (c) 2D Strange attractor

Fig 14: Stranger attractors for the structure Eq.(17) for $b = d = 1$, $\alpha = 2.5$, and $\rho = 1.3$ with beginning value $(0.52, 0.12)$.

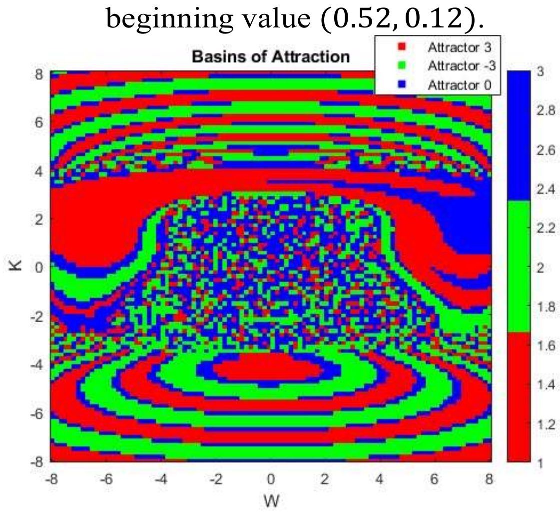

Fig 15: Basins of attraction for the structure Eq.(17) for $b = 1$, $d = 2$, $\alpha = 2.5$, and $\rho = 1.3$.

10. Modulation instability analysis

Modulation instability (MI) [7, 12] leads to dispersion and nonlinear impacts in various nonlinear systems. We use linear stability investigation to study the MI analysis of the governing Eq.(1). Assume the example where the altered steady-state result of Eq.(1) is given by:

$$w = \left[\sqrt{a} + P(x,t)\right]e^{i\phi}, \phi = at, \tag{18}$$

where ϕ is the phase ingredient, a is the normalized optical power, and $P \ll a$. Analysis of linear stability is used to study the alteration of $P(x,t)$. When Eq.(18) is linearized and inserted into Eq.(1), we get

$$iP_t + P_{xx} + a(P + P^*) = 0. \tag{19}$$

The complex conjugate function is indicated by $*$. Let's say that the answer to Eq.(19) is as follows:

$$P(x,t) = r_1\, e^{i(lx-mt)} + r_2\, e^{-i\,(lx-mt)}, \tag{20}$$

where m is the instability frequency and l is the normalized wave number.

We derive two equations in r_1 and r_2 by imposing ansatz Eq.(20) into Eq.(19), and split the coefficients of $e^{i(lx-mt)}$ and $e^{-i\,(lx-mt)}$ which are defined as

$$(-m - l^2 + a)r_2 + ar_1 = \quad 0, (m - l^2 + a)r_1 + ar_2 = 0. \tag{21}$$

Eq.(21) provides the coefficient matrix of r_1 and r_2 in the underneath pattern

$$\begin{bmatrix} -m - l^2 + a & a \\ a & m - l^2 + a \end{bmatrix} \begin{bmatrix} r_1 \\ r_2 \end{bmatrix} = \begin{bmatrix} 0 \\ 0 \end{bmatrix}. \tag{22}$$

A barrier must disappear to ensure a nontrivial solution to the coefficient matrix. Consequently, increasing the determinant yields the dispersion relation, which is

$$(-m - l^2 + a)(m - l^2 + a) - a^2 = 0. \tag{23}$$

The dispersion relation Eq.(23) for m can be solved as follows:

$$m = \pm\sqrt{l^4 - 2al^2}. \tag{24}$$

This formula calculates steady-state stability using wave number l and the normalized optical power a. If $l^4 - 2al^2 \geq 0$, then m is real for all values of l, and the steady state is stable for minor changes. Again, the steady-state solution is probably unstable if $l^4 - 2al^2 < 0$, that is, m is imaginary, and the change spreads quickly. As a result, the following conditions must be satisfied for modulation instability:

$$l^4 - 2al^2 < 0. \tag{25}$$

Thus, the growth rate of MI gain spectra $G(l)$ can be described by

$$G(l) = 2\, Im(m) = 2\, Im(\pm\sqrt{l^4 - 2al^2}). \tag{26}$$

Under different values of the model parameters, **Fig.16** displays the range of modulation instability (MI) gains. The MI gain is highly sensitive to both the sign and strength of the normalized optical power a. A positive a is necessary to guarantee the occurrence of MI gain. **Fig.16a** demonstrates the MI growth rates for various selections of a, while **Fig.16b** shows the evolution of the gain spectrum for its 3D view.

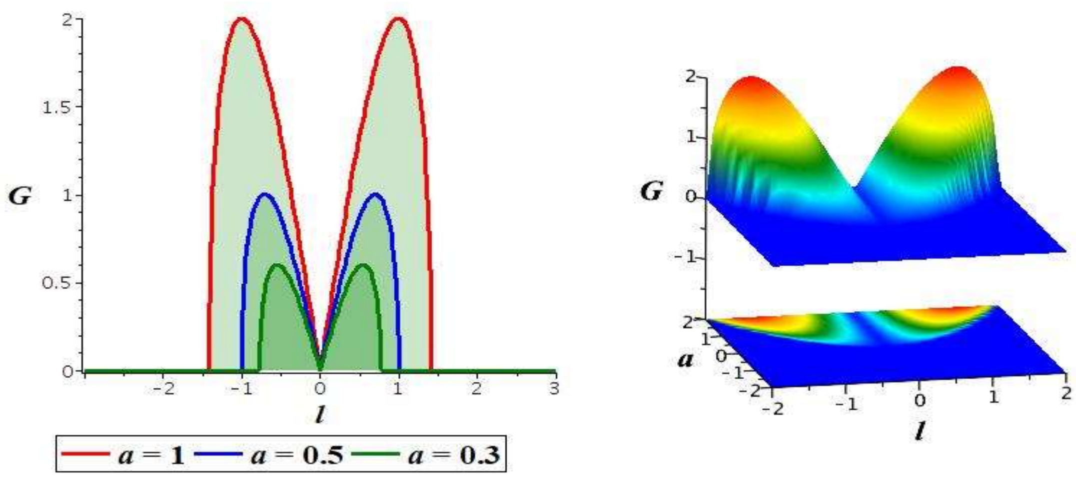

(a) (b)

Fig 16: Modulation instability plot of Eq.(26) (a) 2D plot, (b) 3D plot.

11. Comparison and results novelty

This portion highlights the novelty of our results by comparing them with previous studies. Alam et al. [27] used the modified (G'/G)-expansion method, whereas we employed the unified solver approach. When we look at their findings alongside ours, we notice that they match a specific example of our broader results. For example, if we take the particular values $g = 0$ and $d = -b^3 - \frac{\lambda^2}{2} + 2\mu$ in our generalized result $w_{1,2}$ with arbitrary constants b, λ, and μ, we obtain Alam et al.'s solution (26). Additionally, by taking some specific values of our other results $w_{3,4}$, $w_{5,6}$, $w_{7,8}$, and $w_{9,10}$, we obtain Alam et al.'s findings (25), (24), (23), and (22), respectively. Therefore, we can say that our result is more generalized than theirs. We use several complex methods, including modulation instability, Lyapunov exponents, recurrence plots, strange attractors, bifurcation analysis, and chaos detection. Our effective method is better than past techniques explaining how nonlinear waves behave. This demonstrates the broad applicability of our findings.

12. Limitations and future works

The model deals with cubic nonlinearity and areas that are only slightly affected by nearby points, which makes it less useful because of unrealistic conditions and limited computing precision. Future research can explore stronger nonlocal effects, more complex systems, managing chaos, and applying this framework to quantum and plasma systems. Studying chaos in the equation could open new research possibilities, like looking into Lyapunov exponents, strange attractors, and multistability. Future research should use computer simulations and experiments to test these ideas. It can also be looked at by adding noise, changing factors over time, or outside influences to understand better how the equation works in real situations. This research could enhance its applicability in science and engineering.

13. Conclusion

We have effectively used the Schrödinger equations with cubic nonlinearity to study bifurcation, chaos, and solitons in detail, enhancing our understanding of quantum mechanics, superconductivity, optics, and plasma physics. We have used the unified solver approach to analyze the soliton output of the specified equation. We include modulation instability which leads to dispersion and nonlinear impacts in various nonlinear systems. To investigate bifurcation extensively, we establish a planner dynamical system taking the Galilean conversion. We then apply diverse chaos detection processes to pinpoint the chaotic state within the governing model. Therefore, our implemented procedures are effective and can enhance our understanding of modern science and technology, providing valuable insights for future research.

Competing interests: The authors declare that they have no conflicts of interest to report regarding the present study.

Author's contributions: Md. Shahidur Rahaman: Methodology, Software, Writing-original draft. **Mohammad Nazrul Islam:** Writing-review & editing, Supervision, Validation. **Mohammad Safi Ullah:** Conceptualization, Formal Analysis, Supervision, Writing-review & editing. All authors have read and agreed to publish the manuscript.

Funding: The author(s) received no external funding for this study.

Data Availability and Materials: All data generated or analysed during this study are included in this published article.

References

[1] Naher, H., Abdullah, F.A.: New generalized (G′/G)-expansion method to the Zhiber-Shabat equation and Liouville equations, J Phys: Conference Series. **890**, 012018 (2017).

[2] Ganie, A.H., Wazwaz, A.M., Seadawy, A.R., Ullah, M.S., Roshid, H.O., Afroz, H.D., Akter, R.: Application of three analytical approaches to the model of ion sound and Langmuir

waves. Pramana J Phys. **98**, 46 (2024).
[3] Seadawy, A.R., Arshad, M., Lu, D.: The weakly nonlinear wave propagation theory for the Kelvin–Helmholtz instability in magnetohydrodynamics flows. Chaos Solitons Fract. **139**, 110141 (2020).
[4] Akram, G., Mahak, N.: Application of the first integral method for solving (1+1) dimensional cubic-quintic complex Ginzburg–Landau equation, Optik. **164**, 210–217 (2018).
[5] Yan, X.W., Tian, S.F., Dong, M.J., Zou, L.: Bäcklund transformation, rogue wave solutions and interaction phenomena for a (3+1)-dimensional B-type Kadomtsev–Petviashvili–Boussinesq equation, Nonlinear Dyn. **92**(2), 709–720 (2018).
[6] Baskonus, H.M., Guirao, J.L.G., Kumar, A., Causanilles, F.S.V., Bermudez, G.R.: Regarding new traveling wave solutions for the mathematical model arising in telecommunications. Adv Math Phys. **2021**, 5554280 (2021).
[7] Roshid, M.M., Rahman, M., Uddin, M., Roshid, H.O.: Modulation instability, analytical, and numerical studies for integrable time fractional nonlinear model through two explicit methods, Adv Math Phys **2024**, 6420467 (2024).
[8] Ullah, M.S., Ali, M.Z., Roshid, H.O.: Bifurcation analysis and new waveforms to the first fractional WBBM equation. Sci Rep. **14**, 11907 (2024).
[9] Ullah, M.S., Ali, M.Z., Roshid, H.O.: Bifurcation analysis and new waveforms to the fractional KFG equation, Part Differ Equ Appl Math. **10**, 100716 (2024).
[10] Gu, M., Li, J., Liu, F., Li, Z., Peng, C.: Propagation of traveling wave solution of the strain wave equation in microcrystalline materials, Open Phys, **22**(1), 20240093 (2024).
[11] Gu, M., Liu, F., Li, J., Peng, C., Li, Z.: Explicit solutions of the generalized Kudryashov's equation with truncated M-fractional derivative. Sci Rep. **14**, 21714 (2024).
[12] Zhang, K., Cao, J., Lyu, J.: Dynamic behavior and modulation instability for a generalized nonlinear Schrödinger equation with nonlocal nonlinearity, Phys Scr. **100**, 015262 (2025).
[13] Roshid, M.M., Rahman, M.M.: Bifurcation analysis, modulation instability and optical soliton solutions and their wave propagation insights to the variable coefficient nonlinear Schrödinger equation with Kerr law nonlinearity, Nonlinear Dyn. **112**, 16355-16377 (2024).
[14] Djaouti, A.M., Roshid, M.M., Abdeljabbar, A., Al-Quran, A.: Bifurcation analysis and solitary wave solution of fractional longitudinal wave equation in magneto-electro-elastic

(MEE) circular rod, Results Phys **64**, 107918 (2024).
[15] Roshid, M.M., Rahman, M.M., Roshid, H.O.: Effect of the nonlinear dispersive coefficient on time-dependent variable coefficient soliton solutions of the Kolmogorov-Petrovsky-Piskunov model arising in biological and chemical science, Heliyon **10**(11), e31294 (2024).
[16] Ullah, M.S., Roshid, H.O., Ali, M.Z.: New wave behaviors and stability analysis for the (2+1)-dimensional Zoomeron model. Opt Quant Electron. **56**, 240 (2024).
[17] Mostafa, M., Ullah, M.S.: Soliton outcomes and dynamical properties of the fractional Phi-4 equation, AIP Advances, **15**(1), 015105 (2025).
[18] Akter, M., Ullah, M.S., Wazwaz, A.M., Seadawy, A.R.: Unveiling Hirota-Maccari model dynamics via diverse elegant methods. Opt Quant Electron **56**, 1127 (2024).
[19] Alam, N., Ullah, M.S., Nofal, T.A., Ahmed, H.M., Ahmed, K.K., AL-Nahhas, M.A.: Novel dynamics of the fractional KFG equation through the unified and unified solver schemes with stability and multistability analysis, Nonlin Eng, **13**(1), 20240034 (2024).
[20] Alam, N., Akbar, M.A., Ullah, M.S., Mostafa, M., Dynamic waveforms of the new Hamiltonian amplitude model using three different analytic techniques. Indian J Phys **98**, 1-8 (2024).
[21] Ganie, A.H., Rahaman, M.S., Aladsanic, F.A., Ullah, M.S., Bifurcation, chaos, and soliton analysis of the Manakov equation, Nonlinear Dyn, **113**, 1-15 (2025).
[22] Yasin, F., Arshad, M., Farid, G., Hoseinzadeh, M.A., Rezazadeh, H.: W-shape and abundant of other solitary wave solutions of the positive Gardner Kadomtsov–Petviashivilli dynamical model with applications. Opt Quant Electron **56**, 1214 (2024).
[23] Roshid, M.M., Uddin, M., Hossain, M.M.: Investigation of rogue wave and dynamic solitary wave propagations of the M-fractional (1+ 1)-dimensional longitudinal wave equation in a magnetic-electro-elastic circular rod, Indian J Phys. **99**, 1-17 (2024).
[24] Roshid, M.M., Rahman, M.M., Roshid, H.O., Bashar, M.H.: A variety of soliton solutions of time M-fractional: Non-linear models via a unified technique, Plos One. **19**(4), e0300321 (2024).
[25] Ullah, M.S., Roshid, H.O., Ali, M.Z.: Bifurcation analysis and new waveforms to the fractional KFG equation, Partial Differ Equ Appl Math. **10**, 100716 (2024).
[26] Yang, L., Rahman, M.U., Khan, M.A.: Complex dynamics, sensitivity analysis and

soliton solutions in the (2+1)-dimensional nonlinear Zoomeron model. Results Phys. **56**, 107261 (2024).
[27] Alam, M.N., İlhan, O.A., Akash, H.S., Talib, I.: Bifurcation analysis and new exact complex solutions for the nonlinear Schrödinger equations with cubic nonlinearity. Opt Quant Electron. **56**, 302 (2024).
[28] Rehman, H.U, Iqbal, I., Zulfiqar, H., Gholami, D., Rezazadeh, H., Stochastic soliton solutions of conformable nonlinear stochastic systems processed with multiplicative noise. Physics Letters A. **486**, 129100 (2023).
[29] Kazmi, S.S., Jhangeer, A., Raza, N., Alrebdi, H.I., Abdel-Aty, A.H., Eleuch, H.: The analysis of bifurcation, quasi-periodic and solitons patterns to the new form of the generalized q-deformed sinh-Gordon equation. Symmetry. **15**, 1324 (2023).
[30] Li, Z., Lyu, J., Hussain, E.: Bifurcation, chaotic behaviors and solitary wave solutions for the fractional twin-core couplers with Kerr law non-linearity. Sci Rep. **14**, 22616 (2024).
[31] Li, Z., Zhao, S.: Bifurcation, chaotic behavior and solitary wave solutions for the Akbota equation. AIMS Math. **9**(8), 22590-22601 (2024).
[32] Ali, K.K., Faridi, W.A., Yusuf, A., Rahman, M.A., Ali, M.R.: Bifurcation analysis, chaotic structures and wave propagation for nonlinear system arising in oceanography. Results Phys. **57**, 107336 (2024).
[33] Sprott, J.C.: A proposed standard for the publication of new chaotic systems. Int J Bifur Chaos. **21**(9), 2391-2394 (2011).
[34] Jhangeer, A., Jamal, T., Talafha, A.M., Riaz, M.B.: exploring travelling wave solutions, bifurcation, chaos, and sensitivity analysis in the (3+1)-dimensional gKdV-ZK model: A comprehensive study using Lie symmetry methodology. Results Eng. **22**, 102194 (2024).
[35] Jhangeer, A., Rezazadeh, H., Seadawy, A.R.: A study of travelling, periodic, quasi-periodic and chaotic structures of perturbed Fokas-Lenells model. Pramana J Phys. **95**, 41 (2021).
[36] Li, Z., Hu, H.: Chaotic pattern, bifurcation, sensitivity and traveling wave solution of the coupled Kundu-Mukherjee-Naskar equation. Results Phys. **48**, 106441 (2023).